

Experimental Two-dimensional Quantum Walk on a Photonic Chip

Hao Tang^{1,2}, Xiao-Feng Lin^{1,2}, Zhen Feng^{1,2}, Jing-Yuan Chen¹, Jun Gao^{1,2},
Xiao-Yun Xu^{1,2}, Yao Wang^{1,2}, Lu-Feng Qiao^{1,2}, Ai-Lin Yang^{1,2} and Xian-Min Jin^{1,2,3}

¹*State Key Laboratory of Advanced Optical Communication Systems and Networks,
Institute of Natural Sciences & Department of Physics and Astronomy,
Shanghai Jiao Tong University, Shanghai 200240, China*

²*Synergetic Innovation Center of Quantum Information and Quantum Physics,
University of Science and Technology of China, Hefei, Anhui 230026, China*

³*xianmin.jin@sjtu.edu.cn*

Quantum walks, in virtue of the coherent superposition and quantum interference, possess the exponential superiority over its classical counterpart in applications of quantum searching and quantum simulation. A straightforward physical implementation involving merely photonic source, linear evolution network and detection make it very appealing, in light of the stringent requirements of universal quantum computing. The quantum enhanced power is highly related to the state space of quantum walks, which can be expanded by enlarging the dimension of evolution network and/or photon number. Increasing photon number is considerably challenging due to probabilistic generation of single photons and multiplicative loss. Here we demonstrate a two-dimensional continuous-time quantum walk by using the external geometry of photonic waveguide arrays, rather than inner the degree of freedom of photons. Using femtosecond laser direct writing, we construct a large-scale three-dimensional structure which forms a two-dimensional lattice with up to 49×49 nodes on a photonic chip. We demonstrate the quantum transport properties via observing the ballistic evolution pattern and the variance profile, which agree well with simulation results for quantum walks. We further reveal the transient nature of the walk from our implementation, suggesting a higher dimension. An architecture that allows free evolvment in all directions and large scale, combing with defect and disorder control, may bring up powerful and versatile quantum walk machines for classically intractable problems.

I. INTRODUCTION

Quantum walks (QWs), the quantum analogue of classical random walks^{1,2}, demonstrate remarkably different behaviours comparing to classical random walks, mainly due to the superposition of the quantum walker in its paths. This very distinct feature leads the quantum walks to be a stunningly powerful approach to quantum information algorithms³⁻⁷, and quantum simulation for various systems⁸⁻¹⁰. For instance, theoretical research

has revealed that QWs that propagate in one dimension (1D) possess superior transport properties to 1D classical random walks¹¹, and the coherence in QWs is crucial in simulating the energy transport issue in the photosynthetic process^{9,10}. The potential of applying QWs in machine learning algorithms such as artificial neural network⁶ also draw wide attention from multidisciplinary researchers. Inspired by the prospects of QWs, many endeavours have been made to realize QWs in different physics systems, including nuclear magnetic resonance¹², trapped neutral atoms¹³, trapped ions¹⁴, and optics system¹⁵⁻¹⁷.

However, these experimental implementations reveal a very evident limitation, that the realised quantum walk is normally of only one dimension, and the evolving scale of QWs remains very small. Simple demonstration of 1D QW could not suffice the ever growing demand for further speed-up of certain quantum algorithms, and simulation of quantum systems of a much higher complexity^{18,19}. In the spatial search algorithm, a quantum walk outperforms its classical counterparts only when the dimension is higher than one²⁰; In the simulation of graphene, photosynthesis, or neural network systems, these complex networks always intuitively have high dimensions. Experimental research on higher-dimensional QWs becomes indispensable, and a few attempts having covered 2D QWs in experiments are worth noted. A discrete-time 2D quantum walk was achieved in the fibre network system by dynamically controlling the time interval of two walkers²¹, in the so-called delayed-choice scheme²², or using two walkers sharing coins²³. They ingeniously use two walkers acting on 1D graph to represent one walker on 2D lattice, and a 2D lattice does not physically occur. A quasi-2D continuous-time quantum walk was explored in the waveguide coupled in a “Swiss cross” arrangement¹⁸, where photons could not freely propagate in the diagonal and many arbitrary directions as they suppose to do in the 2D array.

In this paper, we present the experimental simulation for 2D continuous-time quantum walks based on the 2D waveguide array. We analyse the transport property and the recurrent property, measured from the variance and the probability from the initial waveguide, respectively. We observed unique features for two-dimensional QWs that differ from both classical random walks and QWs of one-dimension.

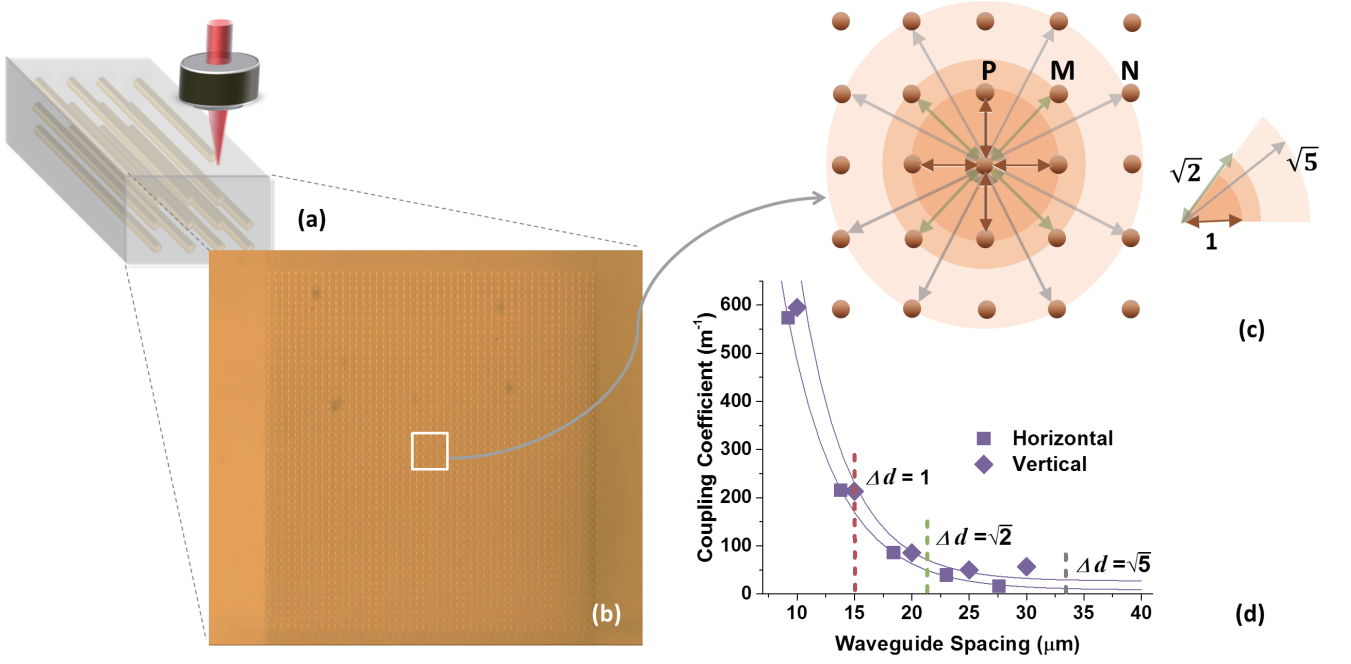


FIG. 1: **The photonic waveguide array.** (a) Schematic diagram of waveguide fabrication using the femtosecond laser writing techniques. (b) Cross section of a 2D waveguide array studied in this experiment. (c) Schematic diagram of one waveguide coupling to other waveguides in the 2D array, and (d) the corresponding coupling coefficient C for different centre-to-centre waveguide spacings in horizontal and vertical directions.

II. MAIN

Photons propagating through the coupled waveguide arrays can be described by the Hamiltonian:

$$H = \sum_i \beta_i a_i^\dagger a_i + \sum_{i \neq j} C_{i,j} a_i^\dagger a_j \quad (1)$$

where β_i is propagating constant in waveguide i , $C_{i,j}$ is the coupling strength between waveguide i and j . When $i = j$, one can define diagonal entries $C_{i,i} = \beta_i$. For a uniform array, all β_i is regarded equal to β , and $C_{i,j}$ that mainly depends on waveguide spacing can be obtained using a coupled mode approach²⁴.

In our implementation, we fabricate two-dimensional waveguide arrays via femtosecond laser writing techniques²⁵ (see Figure 1a and Methods). The waveguides are written in different depths of the borosilicate glass so that they form a 2D array from the cross-section view (Figure 1b). The centre-to-centre spacing between two nearest waveguides (defined as spacing unit here) is set to be $15 \mu\text{m}$. For these 2D waveguides in our implementation, each waveguide is involved into complicated coupling with surrounded waveguides shown in Figure 1c. Δd is the normalised waveguide spacing defined as the ratio of the spacing and the spacing unit, e.g., Δd for Waveguide P , M and N (as marked in Fig.1c) are $1, \sqrt{2}$ and $\sqrt{5}$, respectively. We've obtained the value of C for different centre-to-centre

waveguide spacings along the horizontal direction and the vertical direction, as shown in Figure 1d. The value of C decays exponentially as waveguide spacing increases, and the values for the horizontal direction deviate no more than 10% from those for the vertical direction, suggesting a good uniformity in the 2D waveguide array. We regard the values of C for the inclined directions as the average of the values for horizontal and vertical directions at the corresponding spacing.

For a quantum walk that evolves along the waveguide, the propagation length z is proportional to the propagation time by $z = ct$, where c is the speed of light, and hence all terms that are a function of t would use z instead in this paper for simplicity. The wavefunction that evolves from an initial wavefunction satisfies²⁶:

$$|\Psi(z)\rangle = e^{-iHz} |\Psi(0)\rangle \quad (2)$$

Where $|\Psi(z)\rangle = \sum_j j a_j(z) |j\rangle$, and $|a_j(z)|^2 = |\langle j | \Psi(z) \rangle|^2 = P_j(z)$ respectively. $|a_j(z)|^2$ and $P_j(z)$ is the probability of the walker being found at waveguide j at the propagation length z . In experiment, we observe the dynamics by injecting a vertically polarised 780nm laser beam into the central waveguide. Such classical optics could represent a single walker as the former has shown equivalence in its coherent processes with that in quantum mechanics^{27,28}, and it has been commonly adopted in quantum information, such as to demonstrate Grover's quantum search algorithm²⁹ and a discrete-time 2D quantum walk²¹.

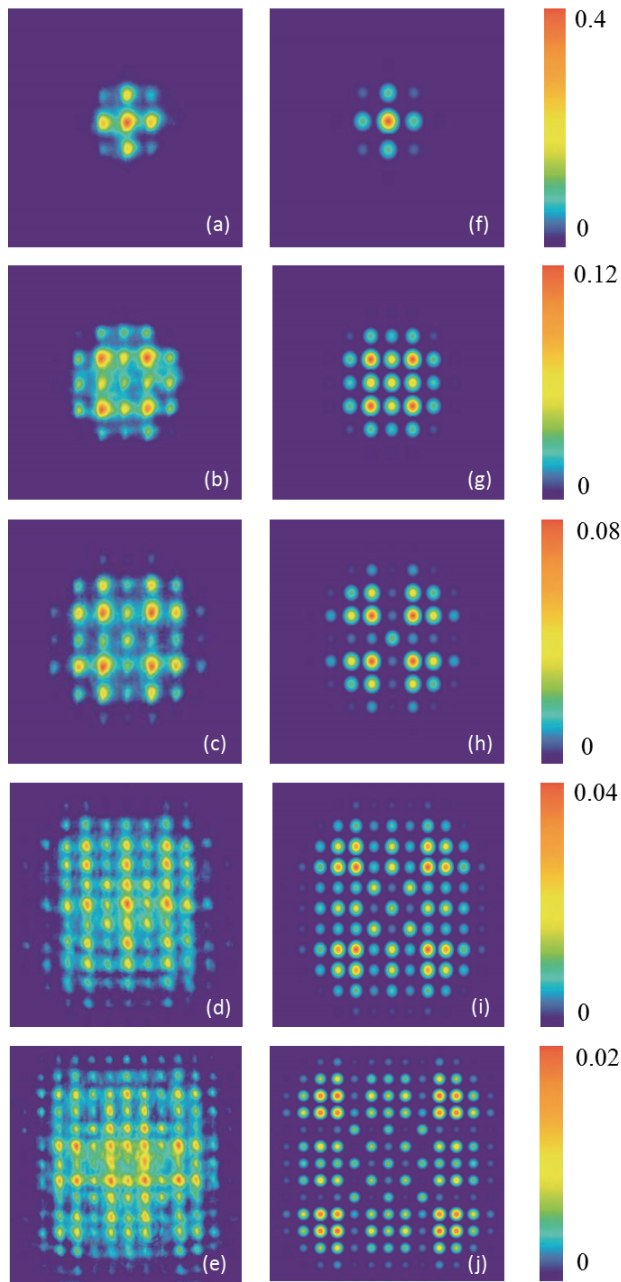


FIG. 2: **2D quantum walks of different propagation lengths.** (a-e) Experimentally obtained probability distribution and (f-j) theoretical probability distribution. The propagation lengths are: 1683 μm for (a) and (f), 3183 μm for (b) and (g), 4183 μm for (c) and (h), 6752 μm for (d) and (i), and 8752 μm for (e) and (j).

The probability distribution of the walker in these 2D photonic lattice of different propagation lengths are collected, from both experimental measurements and theoretical simulations (see Figure 2 and Methods). Clearly, the intensity peaks always emerge at the diagonal directions, and they move further in these directions when the

propagation length z increases. The experimental results of the 2D QW agree well with the theoretical results at corresponding small z , and display a bit localisation at large z for which we attribute to the effect induced by lattice disorder and decoherence.

A. The transport properties of quantum walks

Quantum walks have unique transport properties, which could be examined from the variance against the propagation length:

$$\sigma(z)^2 = \frac{\sum_{i=1}^N \Delta d_i^2 P_i(z)}{\sum_{i=1}^N P_i(z)} \quad (3)$$

where $P_i(z)$ is the probability of the walker in waveguide i at propagation length z , and Δd_i is the normalised spacing between waveguide i and the central waveguide where the laser beam is injected into. The variance goes up when the propagation length increases³⁰. Plotting the variance-propagation length relationship with double-logarithmic axes, the ballistic 1D quantum walk is known for yielding a straight line with slope 2, while the diffusive 1D classical random walk results in a straight line with slope 1, i.e., QW transports quadratically faster than the classical random walk^{31,32}.

The variance for 1D QWs in theory, 2D QWs in theory and 2D QWs in this experiment are obtained and presented in Figure 3a. All QWs follow the same curve of C (Figure 1b) and have the same waveguide spacing unit as 15 μm . The lattice scale for all quantum walks is up to 49×49 nodes, and thus large enough to ignore boundary effects. For 2D QWs, the experimental results agree well with the theoretical results. The variance derived from 1D QWs in theory goes below that from 2D QWs in theory, as a walker can move in more directions in 2D than in 1D. However, the variance for all these quantum walks follows the trend of slope 2 rather than slope 1. Ballistic spreading is universal for quantum walks in both 1D and 2D, and this distinguishes them from diffusive classical random walks.

Projecting the evolution patterns of a 2D quantum walk and a 2D classical random walk onto x axis and y axis (Fig 3.b and c), the 2D random walk in 2D Gaussian distribution³³ corresponds to the projection profiles in 1D Gaussian distribution, while the projection profiles for 2D QWs have a ballistic shape similar to 1D QWs. I.e., the intensity peaks in random walks always remain in the centre, but those in QWs always move to all frontiers, causing a larger variance for QWs.

B. The recurrent properties of quantum walks

We further investigate the difference between quantum walks in 2D and 1D. The former represents a more complex system, and such a different nature could be gauged

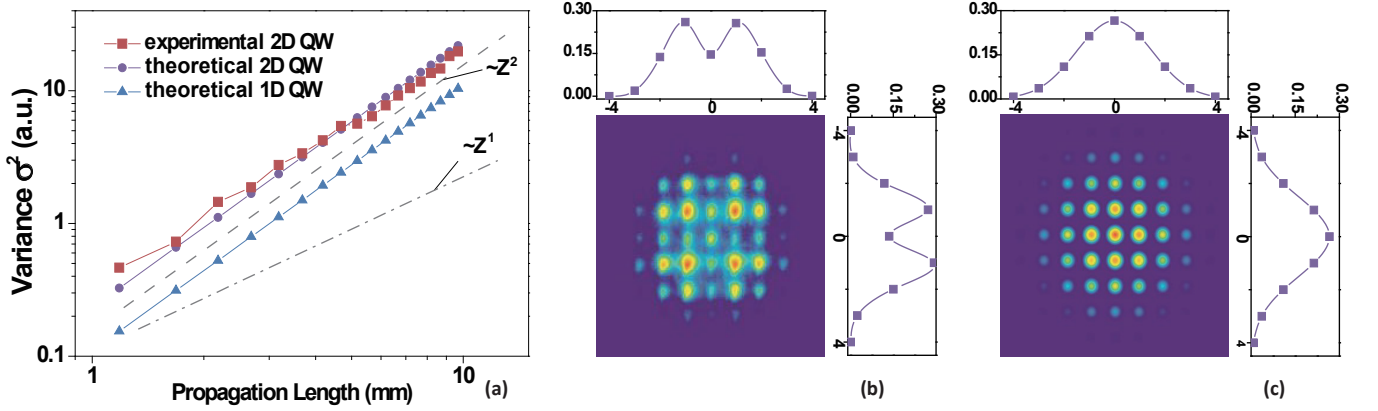


FIG. 3: **The transport properties of quantum walks.** (a) The variance against propagation length for experimental 2D QWs, theoretical 2D QWs and theoretical 1D QWs. (b) A light evolving pattern from the experiment for a 2D QW at propagation length $z=4183\mu\text{m}$ and its projection profile onto x and y axis. (c) A light evolving pattern from the simulation for a 2D Gaussian distribution with a sigma of 1.5 spacing units and its projection profile onto x and y axis.

by $P_0(z)$ and Pólya number, two indices that concern the recurrent properties of a walker in a network.

$P_0(z)$, the probability of a walker being found at the initial waveguide after a propagation length z , is plotted in Figure 4a. For 2D QWs in experiment and in theory, and 1D QWs in theory, they all have a decreasing $P_0(z)$ as z increases, but the asymptotic lines for 2D QWs and 1D QWs are z^{-2} and z^{-1} , respectively, and the oscillation of $P_0(z)$ for 2D QWs is much less severe. A walker in a 2D lattice can evolve away from the original site much easier and is less likely to move back (with a smaller oscillation).

A system can be judged to be recurrent or transient depending on the Pólya number, through the definition^{34,35}:

$$P = 1 - \prod_{m=1}^{\infty} [1 - P_0(z_m)] \quad (4)$$

where z_m is a set of propagation lengths sampled periodically³⁵. When the Pólya number is 1, a system is recurrent, because $P_0(z_m)$ can always be a large value to make $\prod_{i=1}^{\infty} [1 - P_0(z_m)]$ close to zero, while for a transient system, $P_0(z_m)$ quickly drops to a very marginal value so the Pólya number would be smaller than one^{36,37}.

2D QWs in experiment and in theory, and 1D QWs in theory show a Pólya number approaching 0.891, 0.912 and 0.998, respectively (see Figure 4b). Clearly, the 2D QW is much less inclined to be recurrent than 1D QW. Further interpretation³⁵ comes from the asymptotic features z^{-d} . It has been pointed out that transient systems tend to have a value of d larger than one, while d for recurrent systems would be equal to or go below 1. From Figure 4a, the 2D quantum walks in experiment and in theory both follow an asymptotic line z^{-2} , revealing the transient nature for these 2D continuous-time quantum walks in our implementation. We for the first time measure the transient nature of a 2D quantum walk in exper-

iment, which makes it different from all experimentally realised quantum walks that were either in 1D or in 2D with limited scales.

III. DISCUSSION

Here, we have demonstrated strong capacity in achieving large-scale three-dimensional photonic chip that is crucial for our implementation of 2D continuous-time quantum walk. We increase the dimensionality by the geometry of the walker. Even with single walker in our experiment, the 2D lattice can reach a scale with up to thousands of quantum evolution paths, which would be promptly exploited for real-life quantum applications.

We do not simply enlarge the size, but also manage to control each waveguide independently with high precision. Since our scheme is spatial 2D, we could introduce defect, disorder and topological structure in a programmable way when we fabricate the evolution system. Through these we are able to extend the issue of localisation in quantum walks to higher dimensions³⁸. We could also explore topological photonics and the simulation of quantum open systems in photonic lattices³⁹.

Further, we would go beyond two dimensions through various ways. The time-variance term could be introduced along the evolving direction to create an extra dimension. Together with the inner degrees of freedom of photon itself, a highly hyper-dimensional QWs can be developed to push the capacity for quantum tasks. For issues such as quantum walks in bosonic and fermionic behaviours⁴⁰, multi-particle entanglement and evolution, etc., Multi-photon source interfaced to the robust and precise photonic chips could give the research of high dimension quantum systems an instant boost, and demonstrate its strong potential for quantum simulation in a highly complex regime.

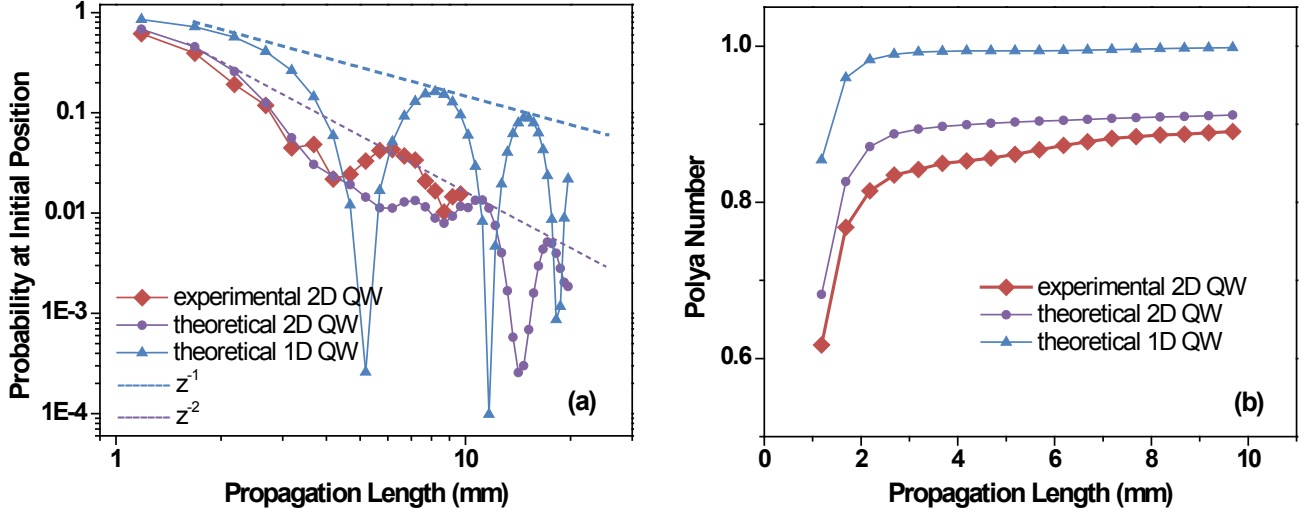


FIG. 4: **The recurrent properties.** (a) Probability at the initial position against propagation length for experimental 2D QWs, theoretical 2D QWs and theoretical 1D QWs. (b) Pólya number for experimental 2D QWs, theoretical 2D QWs and theoretical 1D QWs..

Methods

Waveguide preparation. Waveguide arrays were prepared by directing a femtosecond laser (10W, 1026 nm, 290 fs pulse duration, 1 MHz repetition rate and up-converted 513 nm working frequency) into an spatial light modulator (SLM) to create burst trains onto a borosilicate substrate with a 50X objective lens (numerical aperture: 0.55) at a constant velocity of 10 mm/s. Power and SLM compensation were processed to ensure the waveguides to be uniform and depth independent⁴¹. The borosilicate substrate has a cross section size of 20 mm \times 1 mm, and one substrate contains 10 sets of waveguide arrays, each array consisting of 49 \times 49 waveguides and of a cross section size of around 0.72 mm \times 0.72 mm.

Simulation of light field evolution. Solving Eq.(2) requires a matrix exponential method and this yields the light evolving pattern that contains the probabil-

ity matrix for all waveguides. The Pade approximation function⁴² in Matlab is used in the simulation. In the 2D lattice, as shown in Figure 1c, only the coupling for Δd no more than $\sqrt{5}$ is considered, while for waveguides further apart, the coupling effect becomes very marginal and is ignored in theoretical calculations. The calculated probability for each waveguide is then treated to be a Gaussian spot with the spot intensity proportional to the probability, in order to visualise the comparison between the theoretical pattern and the experimental pattern.

Acknowledgements. The authors thank J.-W. Pan for helpful discussions. This research leading to the results reported here was supported by the National Natural Science Foundation of China (No.11374211), the Innovation Program of Shanghai Municipal Education Commission (No.14ZZ020), Shanghai Science and Technology Development Funds (No.15QA1402200), and the open fund from HPCL (No.201511-01). X.-M.J. acknowledges support from the National Young 1000 Talents Plan.

1. Aharonov, Y., Davidovich, L., & Zagury, N. Quantum random walks. *Phys. Rev. A* **48**, 1687 (1993).
2. Childs, A. M., Farhi, E., & Gutmann, S. An example of the difference between quantum and classical random walks. *Quantum Inf. Process* **1**, 35-43 (2002).
3. Ambainis, A. Quantum walks and their algorithmic applications. *Int. J. Quantum Inf.* **1**, 507-518 (2003).
4. Shenvi, N., Kempe, J., & Whaley, K. B. Quantum random-walk search algorithm. *Phys. Rev. A* **67**, 052307 (2003).
5. Childs, A. M., & Goldstone, J. Spatial search by quantum walk. *Phys. Rev. A* **70**, 022314 (2004).
6. Schuld, M., Sinayskiy, I., & Petruccione, F. The quest for a quantum neural network. *Quantum Inf. Process.* **13**, 2567-2586 (2014).
7. Sánchez-Burillo, E., Duch, J., Gómez-Gardenes, J., & Zueco, D. Quantum navigation and ranking in complex networks. *Sci. Rep.* **2**, 605 (2012).
8. Aspuru-Guzik, A., & Walther, P. Photonic quantum simulators. *Nat. Phys.* **8**, 285-291 (2012).
9. Mülken, O., & Blumen, A. Continuous-time quantum walks: Models for coherent transport on complex networks. *Phys. Rep.* **502**, 37-87 (2011).
10. Lambert, N., Chen, Y. N., Cheng, Y. C., Li, C. M., Chen,

- G. Y., & Nori, F. Quantum biology. *Nat. Phys.* **9**, 10-18 (2013).
11. Mülken, O., & Blumen, A. Efficiency of quantum and classical transport on graphs. *Phys. Rev. E* **73**, 066117 (2006).
 12. Du, J., Li, H., Xu, X., Shi, M., Wu, J., Zhou, X., & Han, R. Experimental implementation of the quantum random-walk algorithm. *Phys. Rev. A* **67**, 042316 (2003).
 13. Karski, M., Förster, L., Choi, J. M., Steffen, A., Alt, W., Meschede, D., & Widera, A. Quantum walk in position space with single optically trapped atoms. *Science* **325**, 174-177 (2009).
 14. Schmitz, H., Matjeschk, R., Schneider, C., Glueckert, J., Enderlein, M., Huber, T., & Schaetz, T. Quantum walk of a trapped ion in phase space. *Phys. Rev. Lett.* **103**, 090504 (2009).
 15. Peruzzo, A., Lobino, M., Matthews, J. C. F., Matsuda, N., Politi, A., Poulios, K., Zhou, X.-Q., Lahini, Y., Ismaili, N., Wörhoff, K., Bromberg, Y., Silberberg, Y., Thompson, M. G., & O'Brien, J. L. Quantum walks of correlated photons. *Science* **329**, 1500-1503 (2010).
 16. Biggerstaff, D. N., Heilmann, R., Zecevic, A. A., Gräfe, M., Broome, M. A., Fedrizzi, A., & Kassal, I. Enhancing coherent transport in a photonic network using controllable decoherence. *Nat. Commun.* **7**, 11208 (2016).
 17. Perets, H. B., Lahini, Y., Pozzi, F., Sorel, M., Morandotti, R., & Silberberg, Y. Realization of quantum walks with negligible decoherence in waveguide lattices. *Phys. Rev. Lett.* **100**, 170506 (2008).
 18. Poulios, K., Keil, R., Fry, D., Meinecke, J. D., Matthews, J. C., Politi, A., Lobino, M., Gräfe, M., Heinrich, M., Nolte, S., Szameit, A., & O'Brien, J. L. Quantum walks of correlated photon pairs in two-dimensional waveguide arrays. *Phys. Rev. Lett.* **112**, 143604 (2014).
 19. Gao, J., Qiao, L. F., Lin, X. F., Jiao, Z. Q., Feng, Z., Zhou, Z., Gao, Z. W., Xu, X. Y., Chen, Y., Tang, H., & Jin, X. M. Non-classical photon correlation in a two-dimensional photonic lattice. *Opt. Express* **24**, 12607-12616 (2016).
 20. Tuls, A. Faster quantum-walk algorithm for the two-dimensional spatial search. *Phys. Rev. A* **78**, 012310 (2008).
 21. Schreiber, A., Gábris, A., Rohde, P. P., Laiho, K., Štefáňák, M., Potoček, V., Hamilton, C., Jex, I., & Silberhorn, C. A 2D quantum walk simulation of two-particle dynamics. *Science* **336**, 55-58 (2012).
 22. Jeong, Y. C., Di Franco, C., Lim, H. T., Kim, M. S., & Kim, Y. H. Experimental realization of a delayed-choice quantum walk. *Nat. Commun.* **4**, 2471 (2013).
 23. Xue, P., Zhang, R., Bian, Z., Zhan, X., Qin, H., & Sanders, B. C. Quantum walk of a trapped ion in phase space. *Phys. Rev. A* **92**, 042316 (2015).
 24. Szameit, A., Dreisow, F., Pertsch, T., Nolte, S., & Trnemann, A. Control of directional evanescent coupling in fs laser written waveguides. *Opt. Express* **15**, 1579-1587 (2007).
 25. Davis, K. M., Miura, K., Sugimoto, N., & Hirao, K. Writing waveguides in glass with a femtosecond laser. *Opt. Lett.* **21**, 1729-1731 (1996).
 26. Izaac, J. A., & Wang, J. B. pyCTQW: A continuous-time quantum walk simulator on distributed memory computers. *Comput. Phys. Commun.* **186**, 81-92 (2015).
 27. Spreeuw, R. J. A classical analogy of entanglement. *Found. Phys.* **28**, 361-374 (1998).
 28. Cerf, N. J., Adami, C., & Kwiat, P. G. Optical simulation of quantum logic. *Phys. Rev. A* **57**, R1477 (1998).
 29. Bhattacharya, N., van den Heuvel, H. V. L., & Spreeuw, R. J. C. Implementation of quantum search algorithm using classical Fourier optics. *Phys. Rev. Lett.* **88**, 137901 (2002).
 30. Whitfield, J. D., Rodríguez-Rosario, C. A., & Aspuru-Guzik, A. Quantum stochastic walks: A generalization of classical random walks and quantum walks. *Phys. Rev. A* **81**, 022323 (2010).
 31. Eichelkraut, T., Heilmann, R., Weimann, S., Sttzer, S., Dreisow, F., Christodoulides, D. N., Nolte, S., & Szameit, A. Mobility transition from ballistic to diffusive transport in non-Hermitian lattices. *Nat. Commun.* **4**, 143604 (2013).
 32. Golshani, M., Weimann, S., Jafari, K., Nezhad, M. K., Langari, A., Bahrampour, A. R., Eichelkraut, T., Mahdavi, S. M., & Szameit, A. Impact of loss on the wave dynamics in photonic waveguide lattices. *Phys. Rev. Lett.* **113**, 123903 (2014).
 33. Manouchehri, K., & Wang, J. B. Continuous-time quantum random walks require discrete space. *J. Phys. A: Math. Theor.* **40**, 13773 (2007).
 34. Darázs, Z., Anishchenko, A., Kiss, T., Blumen, A., & Mülken, O. Transport properties of continuous-time quantum walks on Sierpinski fractals. *Phys. Rev. E* **90**, 032113 (2014).
 35. Darázs, Z., & Kiss, T. Control of directional evanescent coupling in fs laser written waveguides. *Phys. Rev. A* **81**, 062319 (2010).
 36. Kollár, B., Štefáňák, M., Kiss, T., & Jex, I. Recurrences in three-state quantum walks on a plane. *Phys. Rev. A* **82**, 012303 (2010).
 37. Štefáňák, M., Jex, I., & Kiss, T. Recurrence and Pólya number of quantum walks. *Phys. Rev. Lett.* **100**, 020501 (2008).
 38. Lahini, Y., Avidan, A., Pozzi, F., Sorel, M., Morandotti, R., Christodoulides, D. N., & Silberberg, Y. Anderson Localization and Nonlinearity in One-Dimensional Disordered Photonic Lattices. *Phys. Rev. Lett.* **100**, 013906 (2008).
 39. Caruso, F., Crespi, A., Ciriolo, A. G., Sciarrino, F., & Osellame, R. Fast escape of a quantum walker from an integrated photonic maze. *Nat. Commun.* **7**, 11682 (2016).
 40. Sansoni, L., Sciarrino, F., Vallone, G., Mataloni, P., Crespi, A., Ramponi, R., & Osellame, R. Two-Particle Bosonic-Fermionic Quantum Walk via Integrated Photonics. *Phys. Rev. Lett.* **108**, 010502 (2012).
 41. Feng, Z., Wu, B. H., Zhao, Y. X., Gao, J., Qiao, L. F., Yang, A. L., Lin, X. F., & Jin, X. M. Invisibility Cloak Printed on a Photonic Chip. *Sci. Rep.* **6**, 28527 (2016).
 42. Moler, C., & Van Loan, C. Nineteen dubious ways to compute the exponential of a matrix. *SIAM Review* **20**, 801-836 (1978).